Ge-on-glass detectors

C.-H. Lin, Y.-T. Chiang, C.-C. Hsu, C.-H. Lee, and C.-F. Huang
Department of Electrical Engineering, National Taiwan University, Taipei 106, Taiwan, Republic of China and Graduate Institute of Electronics Engineering, National Taiwan University, Taipei 106, Taiwan, Republic of China

C.-H. Lai and T.-H. Cheng
Department of Electrical Engineering, National Taiwan University, Taipei 106, Taiwan, Republic of China and Graduate Institute of Electro-Optical Engineering, National Taiwan University, Taipei 106, Taiwan, Republic of China

C. W. Liu[a)]
Department of Electrical Engineering, National Taiwan University, Taipei 106, Taiwan, Republic of China; Graduate Institute of Electro-Optical Engineering, National Taiwan University, Taipei 106, Taiwan, Republic of China; and Graduate Institute of Electronics Engineering, National Taiwan University, Taipei 106, Taiwan, Republic of China

(Received 22 May 2007; accepted 25 June 2007; published online 24 July 2007)

A single crystalline thin film of Ge on glass is fabricated using wafer bonding and smart cut. A simple metal-insulator-semiconductor detector is demonstrated for visible light and telecommunication wavelength. The implantation damage of separated Ge film bonded on glass is removed by chemical etching, and the surface roughness is reduced from 14 to 4 nm. The defect removal reduces the dark current by a factor of 30 and increases the responsivity by a factor of 1.85 at visible wavelength. The responsivity of 0.27 A/W at 1.3 μm wavelength for an unetched device does not increase after damage removal due to the decrease of the absorption layer thickness. © *2007 American Institute of Physics*. [DOI: 10.1063/1.2759982]

Ge with band gap of 0.66 eV and direct band gap of 0.8 eV is a promising detector for a telecommunication wavelength.[1] The Ge layer much thicker than the absorption length is not desirable due to costly Ge layers. Thin Ge photodetectors have been demonstrated by growing Ge on silicon-on-insulator[2,3] and Si (Refs. 4 and 5) substrates. To further reduce the cost, the glass substrate is of great interest. In this letter, we develop Ge-on-glass (GOG) metal-insulator-semiconductor (MIS) photodetectors by wafer bonding and smart cut.[6,7] The simple MIS structure can be easily fabricated without *n* and *p* dopant diffusions or implantations. Crystalline Ge is directly bonded to glass, so the crystalline substrate is not necessary. The Ge substrate can be reused since only a fraction of Ge is cut and bonded to glass. The GOG structure can be etched before the fabrication of the MIS photodetector to reduce the surface roughness and to remove most defects formed during the implantation process. Moreover, GOG MIS photodetectors can be used for the system-on-panel applications.

The *n*-type, Sb doped (001) Ge substrate with a resistivity of 1–30 Ω cm was prepared as a "host" wafer. The hydrogen ions with a dose of 1.5×10^{17} cm^{-2} and the energy of 150 keV were implanted into the host wafer before bonding to form a weakened layer [Step 1 in Fig. 1(a)]. On the other hand, the Corning 7059 glass was prepared as a "handle" wafer. The host wafer and the handle wafer were hydrophilicly cleaned in the $KOH:H_2O$ solution and $NH_4OH:H_2O_2:H_2O$ solution, respectively. After being rinsed in de-ionized water, the implanted side of Ge was in contact with glass substrate, and the Ge/glass pair was initially bonded at the room temperature [Step 2 in Fig. 1(a)]. Then, this pair was annealed at 150 °C for 8 h to strengthen the chemical bonds at the interface between the Ge and the glass, and subsequent annealing at 200 °C for 40 min induces layer transfer along the weakened hydrogen-implanted regions by H_2 blistering [Step 3 in Fig. 1(a)]. The photograph of the GOG structure is shown in Fig. 1(b), where the rectangular area is Ge. According to the cross-sectional transmission electron micrograph (TEM), the thickness of transferred Ge layer is about 1.3 μm (the inset of Fig. 2) and the top of Ge layer (~300 nm) is defective due to the hydrogen implantation.

The surface roughness of the GOG structure was ~14 nm after smart cut. The SC1 solution ($NH_4OH:H_2O_2:H_2O=1:1:7$) is used to etch the Ge (Ref. 8) in order to remove the defective hydrogen implantation region [Step 4 in Fig. 1(a)]. The surface roughness decreases to ~4 nm after etching for 150 s and an ~530 nm Ge layer was etched away.

Al was evaporated on Ge with a ring shape to form the Ohmic contact. The low-temperature (50 °C) oxide with a thickness of ~2 nm was deposited by liquid phase deposition (LPD), and Pt was used as the gate electrode inside the Al ring to form the MIS photodetector.[9] The gate area is 3×10^{-4} cm^2, and the Al contact area is ~0.1 cm^2. Since the Al Ohmic contact has a large area and the barrier height between Al and Ge is small (0.1 eV), the effect of contact resistance is small.[10] The schematic structure of the GOG MIS photodetector is shown in Fig. 2.

At negative bias, the thermal generated electron-hole pairs via defects at the Ge/SiO_2 interface and in the depletion region of Ge are swept separately by the electric field and form the dark current. Under visible light/infrared exposures, the photogenerated electron-hole pairs can also be swept separately and contribute to the photocurrent. The

[a)]Author to whom correspondence should be addressed; electronic mail: chee@cc.ee.ntu.edu.tw

 © 2007 American Institute of Physics
Downloaded 13 Feb 2009 to 140.112.113.225. Redistribution subject to AIP license or copyright; see http://apl.aip.org/apl/copyright.jsp

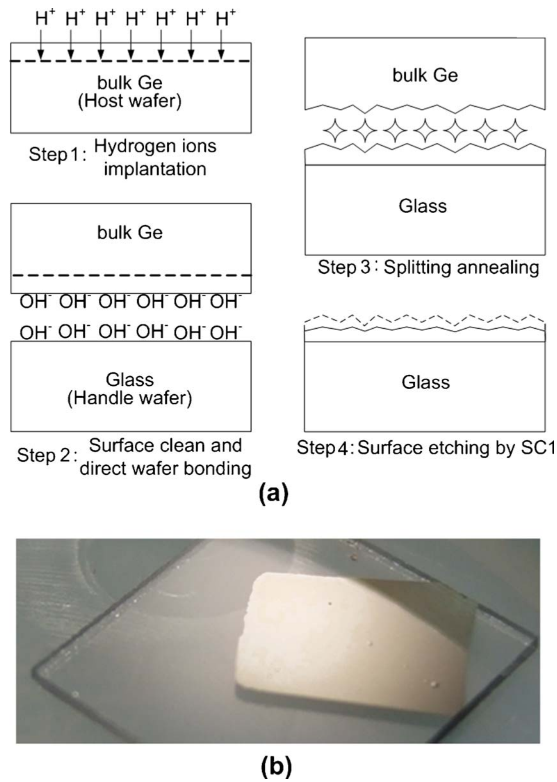

FIG. 1. (Color online) (a) Process flow of Ge-on-glass structure demonstration. (b) Photograph of the thin Ge bonded on glass. The rectangular area is Ge.

LPD oxide can reduce the dark current[11] as compared to Schottky barrier detector and form a deep depletion region in Ge at the negative gate bias for photocarrier collection. The Pt gate with a work function larger than 5 eV can prevent the electron current tunneling from the gate to Ge and lead to lower dark current as compared to the Al gate.

Figure 3 shows the dark currents and photocurrents at 532 nm wavelength of the unetched and etched GOG MIS photodetectors. The dark current of the etched GOG MIS photodetector is reduced by a factor of 30, while the photocurrent is increased by a factor of 1.85. The etched GOG structure has small roughness of 4 nm and the defect density in the depletion region also decreases due to the removal of hydrogen implantation damage. These lead to superior performance of etched devices in terms of dark current and 532 nm photocurrent.

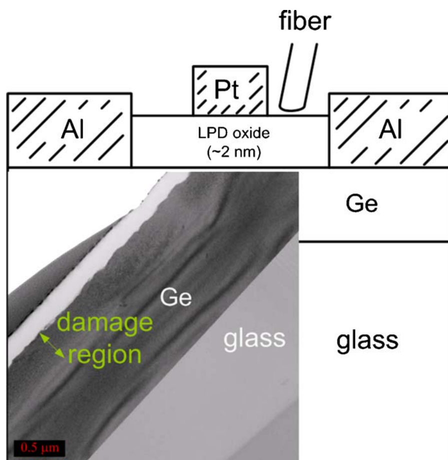

FIG. 2. (Color online) Schematic structure of the Ge-on-glass metal-insulator-semiconductor photodetector. The inset shows the TEM of the Ge-on-glass structure.

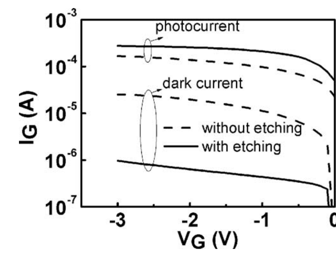

FIG. 3. Dark currents and 532 nm photocurrents of the unetched and etched GOG MIS photodetectors. The etched GOG MIS photodetector has a larger photocurrent and a smaller dark current than the unetched one. The power of light source is 4.2 mW.

The thermal generated electron-hole pairs via defects at the Ge/SiO_2 interface and in the depletion region of Ge decrease after the damage removal, and the dark current consequently decreases. The photogenerated electron-hole pairs should be swept separately to contribute to the photocurrent. However, these photogenerated electrons and holes may recombine via defects without forming the photocurrent (Fig. 4). The defect density decreases after the etching process, and the recombination of photogenerated carriers is significantly suppressed. This phenomenon is especially significant for visible light detection. The etched devices can enhance the responsivity as long as the remaining Ge layer is sufficiently thicker than the absorption depth at exposure wavelength. This is true for 532 and 635 nm wavelengths which have absorption depths of ~20 and ~50 nm, respectively, in Ge (Fig. 5). Note that the remaining Ge after etching is ~770 nm.

The photocurrents of telecommunication wavelength (1.3 and 1.55 μm) are also measured, and the responsivities of the etched and unetched GOG MIS photodetectors are shown in Fig. 5. The responsivities at 1.3 and 1.55 μm of the unetched GOG MIS photodetector are 0.27 and 0.05 A/W, respectively, larger than those of the etched GOG MIS photodetector. The drop of responsivity at 1.3 and 1.55 μm wavelength after etching is due to the insufficient Ge layer thickness (770 nm) as compared to the absorption depths of 1.3 and 22 μm,[1] respectively. Note that there was no antireflection (AR) coating used on the detectors. The further enhancement on responsivity can be expected with the AR coating. A thicker Ge layer that absorbs more infrared at

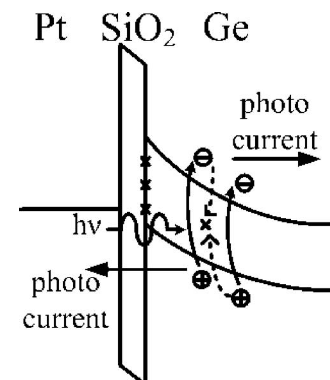

FIG. 4. Mechanism of the photocurrent formation. Photogenerated electrons and holes may recombine via defects without forming the photocurrent.

Downloaded 13 Feb 2009 to 140.112.113.225. Redistribution subject to AIP license or copyright; see http://apl.aip.org/apl/copyright.jsp

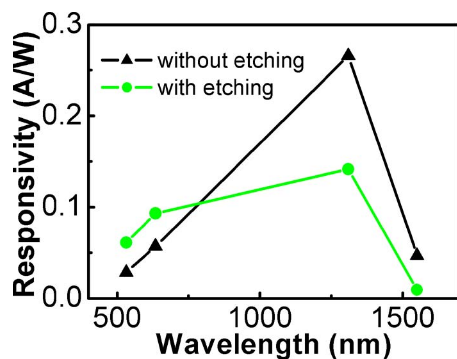

FIG. 5. (Color online) Responsivities of etched and unetched GOG MIS photodetectors at visible light and telecommunication wavelength. The etched GOG MIS photodetector has larger responsivity for visible light but smaller responsivity for telecommunication wavelength.

1.55 μm wavelength can improve the responsivity but the high energy implantation is required. Even 400 keV implantation, the active Ge layer is about 3 μm, which is still too thin as compared to the absorption length. Moreover, such facility is not available now for our experiments. The bonding and etch-back approach[12] may be an alternative to obtain such thick Ge layer ($\sim$22 μm).

In summary, the GOG MIS photodetectors have been demonstrated and the responsivities of visible light and telecommunication wavelength are studied. The etching is proven to be an effective method to remove implantation damage and to reduce the dark current. The remaining Ge after etching should be sufficiently thick as compared to the absorption depth to increase the responsivity.

This work was supported by the National Science Council, Taiwan, R.O.C. under Contract Nos. 95-2221-E-002-357 and 95-2221-E-002-370 and the Applied Materials, Inc.

[1] O. I. Dosunmu, D. D. Cannon, M. K. Emsley, B. Ghyselen, J. Liu, L. C. Kimerling, and M. S. Unlu, IEEE J. Sel. Top. Quantum Electron. **10**, 694 (2004).
[2] G. Dehlinger, S. J. Koester, J. D. Schaub, J. O. Chu, Q. C. Ouyang, and A. Grill, IEEE Photonics Technol. Lett. **16**, 2547 (2004).
[3] M. Rouviere, L. Vivien, X. Le Roux, J. Mangeney, P. Crozat, C. Hoarau, E. Cassan, D. Pascal, S. Laval, J.-M. Fedeli, J.-F. Damlencourt, J. M. Hartmann, and S. Kolev, Appl. Phys. Lett. **87**, 231109 (2005).
[4] L. Colace, G. Masini, F. Galluzzi, G. Assanto, G. Capellini, L. Di Gaspare, E. Palange, and F. Evangelisti, Appl. Phys. Lett. **72**, 3175 (1998).
[5] M. Oehme, J. Werner, E. Kasper, M. Jutzi, and M. Berroth, Appl. Phys. Lett. **89**, 071117 (2006).
[6] Frank Fournel, Hubert Moriceau, Bernard Aspar, Karine Rousseau, Joel Eymery, Jean-Luc Rouviere, and Noel Magnea, Appl. Phys. Lett. **80**, 793 (2002).
[7] Stephen W. Bedell and William A. Lanford, J. Appl. Phys. **90**, 1138 (2001).
[8] M. Heyns, M. Meuris, and M. Caymax, ECS. Trans. **3**, 511 (2006).
[9] B.-C. Hsu, S. T. Chang, T.-C. Chen, P.-S. Kuo, P. S. Chen, Z. Pei, and C. W. Liu, IEEE Electron Device Lett. **24**, 318 (2003).
[10] S. M. Sze, *Physics of Semiconductor Devices*, 2nd ed. (Wiley, New York, 1985), Part 3, p. 304.
[11] C.-H. Lin, C.-Y. Yu, P.-S. Kuo, C.-C. Chang, T.-H. Guo, and C. W. Liu, Thin Solid Films **508**, 389 (2006).
[12] D. Pasquariello and K. Hjort, IEEE J. Sel. Top. Quantum Electron. **8**, 118 (2002).

Downloaded 13 Feb 2009 to 140.112.113.225. Redistribution subject to AIP license or copyright; see http://apl.aip.org/apl/copyright.jsp